

UCLA

UCLA Previously Published Works

Title

Searching for Exoplanets Using a Microresonator Astrocomb.

Permalink

<https://escholarship.org/uc/item/2531p63m>

Journal

Nature photonics, 13(1)

ISSN

1749-4885

Authors

Suh, Myoung-Gyun

Yi, Xu

Lai, Yu-Hung

et al.

Publication Date

2019

DOI

10.1038/s41566-018-0312-3

Peer reviewed



Published in final edited form as:

Nat Photonics. 2019 ; 13: 25–30. doi:10.1038/s41566-018-0312-3.

Searching for Exoplanets Using a Microresonator Astrocomb

Myoung-Gyun Suh¹, Xu Yi¹, Yu-Hung Lai¹, S. Leifer², Ivan S. Grudinin², G. Vasisht², Emily C. Martin³, Michael P. Fitzgerald³, G. Doppmann⁴, J. Wang⁵, D. Mawet^{2,5}, Scott B. Papp⁶, Scott A. Diddams⁶, C. Beichman^{7,*}, and Kerry Vahala^{1,*}

¹T. J. Watson Laboratory of Applied Physics, California Institute of Technology, Pasadena, California 91125, USA

²Jet Propulsion Laboratory, California Institute of Technology, Pasadena, California 91109, USA

³Department of Physics and Astronomy, University of California Los Angeles, Los Angeles, CA 90095, USA

⁴W.M. Keck Observatory, Kamuela, HI 96743, USA

⁵Department of Astronomy, California Institute of Technology, Pasadena, CA 91125, USA

⁶National Institute of Standards and Technology, 325 Broadway, Boulder, Colorado 80305, USA

⁷NASA Exoplanet Science Institute, California Institute of Technology, Pasadena, CA 91125, USA

Abstract

Orbiting planets induce a weak radial velocity (RV) shift in the host star that provides a powerful method of planet detection. Importantly, the RV technique provides information about the exoplanet mass, which is unavailable with the complementary technique of transit photometry. However, RV detection of an Earth-like planet in the ‘habitable zone’¹ requires extreme spectroscopic precision that is only possible using a laser frequency comb (LFC)². Conventional LFCs require complex filtering steps to be compatible with astronomical spectrographs, but a new chip-based microresonator device, the Kerr soliton microcomb^{3–8}, is an ideal match for astronomical spectrograph resolution and can eliminate these filtering steps. Here, we demonstrate an atomic/molecular line-referenced soliton microcomb as a first in-the-field demonstration of microcombs for calibration of astronomical spectrographs. These devices can ultimately provide LFC systems that would occupy only a few cubic centimetres^{9,10}, thereby greatly expanding implementation of these technologies into remote and mobile environments beyond the research lab.

Users may view, print, copy, and download text and data-mine the content in such documents, for the purposes of academic research, subject always to the full Conditions of use: http://www.nature.com/authors/editorial_policies/license.html#terms

*Corresponding author: Kerry Vahala (vahala@caltech.edu) and C. Beichman (chas@ipac.caltech.edu).

Author contributions M.G.S., S.L., G.V., M.P.F., D.M., C.B. and K.V. conceived the experiments. All co-authors designed and performed experiments. M.G.S. and X.Y. built the soliton microcomb setup and EO comb setup with help from S.L., I.S.G., S.D., S.P. and Y.H.L.. G.D. managed operation and experimental interface of the Keck II telescope. E.C.M., J.W., C.B. analyzed NIRSPEC data. C.B. and K.V. supervised the experiment. M.G.S., C.B. and K.V. prepared the manuscript with input from all co-authors.

Competing interests The authors declare no competing interests.

The radial velocity (RV) method (Figure 1) measures periodic Doppler shifts in the stellar spectrum to infer the presence of an orbiting exoplanet¹¹ and relies upon a highly stable and precisely calibrated spectrometer¹². In astronomy, LFCs or simply astrocombs have enabled spectrograph calibration at the few cm s^{-1} level¹³. They do this by providing a spectrally broad ‘comb’ of optical frequencies that are precisely stabilized through the process of self-referencing¹⁴. Self-referencing ensures that both the comb’s spectral line spacing and the common offset frequency of the spectral lines from the origin are locked to a radio frequency standard resulting in a remarkably accurate ‘optical ruler’.

Astrocombs used in prior work^{13,15–20} are derived from femtosecond modelocked lasers and have a comb line frequency spacing that is not resolvable by astronomical spectrographs². This has necessitated the addition of special spectral filters designed to coarsen the line spacing (typically 10–30 GHz)^{13,15–20}. The added complexity of this filtering step has created interest in frequency comb generation by other means that can intrinsically provide a readily resolvable line spacing. For example, electro-optical (EO) modulation provides an alternative approach for direct generation of > 10 GHz comb line spacings^{21,22}. Line referenced EO-astrocomb devices²³ and self-referenced EO-combs^{24,25} have been demonstrated, and more recently, 10 cm/s RV precision using a near-infrared EO-astrocomb²⁶ has been reported. However, these devices require optical filtering to remove amplified phase noise in the wings of the broadened comb. Another optical source that produces wider comb line spacing is in the form of a tiny microresonator-based comb or microcomb^{27,28}. Driven by parametric oscillation and four-wave-mixing²⁹, millimetre-scale versions of these devices have line spacings that are ideally suited for astronomical calibration²⁸. However, until recently microcombs operated in the so-called modulation instability regime of comb formation³⁰ and this severely limited their utility in frequency comb applications.

The recent demonstration of soliton mode-locking in microresonators represents a major turning point for applications of microcombs^{3–8}. Also observed in optical fibre³¹, soliton formation ensures highly stable mode locking and reproducible spectral envelopes. For these reasons soliton microcombs are being applied to frequency synthesis⁹, dual comb spectroscopy^{32–34}, laser-ranging^{35,36}, and optical communications³⁷. Moreover, their compact (often chip-based) form factor and low operating power are ideal for ubiquitous application outside the lab and even in future space-borne instruments. In this work, we demonstrate a soliton microcomb as an astronomical spectrograph calibrator. We discuss the experimental setup, laboratory results and efforts to detect a previously known exoplanet.

The on-site soliton microcomb demonstration was performed at the 10 m Keck II telescope of the W.M. Keck Observatory in order to calibrate the near-infrared spectrometer (NIRSPEC). A secondary goal was to detect the RV signature of the $0.5 M_{\text{Jup}}$ planet orbiting the G3V star HD187123 in a 3.1 day period³⁸. Calibrations and observations were performed during the first half nights of 2017-09-10 and 2017-09-11 (UTC) in the hope of detecting the 70 m s^{-1} semi-amplitude of this planetary signature. As a cross-check, the functionality of the soliton microcomb was compared with a previously-demonstrated line-referenced EO-astrocomb²³. The soliton and EO combs described here operate in the near-infrared (NIR), centred at 1560 nm with a usable breadth of $\sim 250 \text{ nm}$. NIR wavelengths are

avored over visible wavelengths for the study of very cool stars, i.e. the M dwarfs. These comprise about 70 percent of the stars in our galaxy and emit predominantly at long wavelengths^{26,39,40}.

The experimental apparatus for both combs was established in the computer room adjacent to the telescope control room. Both combs were active simultaneously and the output of either one could be fed into the integrating sphere at the input to the NIRSPEC calibration subsystem via single-mode fibre. The switch between the two combs could be carried out in the computer room within less than a minute by changing the input to the fibre without disturbing NIRSPEC itself.

The primary elements of the soliton comb calibration system are detailed in Figure 2a. The LFC light (soliton microcomb or EO comb) is sent to the fibre acquisition unit (light green box) to calibrate the NIRSPEC spectrometer⁴¹. Soliton generation uses a silica microresonator fabricated on a silicon wafer⁴². The resonator featured a 3 mm diameter corresponding to an approximate 22.1 GHz soliton comb line spacing and had an unloaded quality factor of approximately 300 million (see Methods). Figure 2b shows the optical spectrum of the soliton microcomb. The soliton repetition frequency (f_{rep}) was locked to a rubidium-stabilized local oscillator by servo control of the pump power using an AOM so as to vary the soliton repetition rate. Allan deviation measurement of the locked and frequency-divided signal show an instability of 10 mHz at 1000 s averaging time (Figure 2c). The frequency of one of the soliton comb lines is monitored by heterodyne detection with a reference laser, which is locked to a hydrogen cyanide (HCN) absorption line at 1559.9 nm. The resulting offset frequency f_0 is recorded at every second using a frequency counter stabilized to the Rb clock with a time stamp for calibration of the frequency comb over time. For calibration of the frequency comb over time, f_0 was determined over a 20 second averaging time (i.e., acquisition time for a single spectrum) with standard deviation less than 1 MHz. Over this time, the absolute optical frequency of the HCN reference laser has an imprecision of less than 1 MHz²³ (see Methods). Because the soliton repetition rate (i.e., comb line spacing) is frequency locked, the offset frequency imprecision was the principal source of instability in the comb calibration, equivalent to about 1 m s^{-1} of RV imprecision. Finally, the soliton microcomb is spectrally broadened using highly nonlinear optical fibre (see Methods).

Figure 3a shows the echellogram of the soliton microcomb measured by NIRSPEC (8 Echelle orders ranging from 1471 nm to 1731 nm, which represents almost the entire astronomical *H*-band). The raw echellograms were rectified spatially and spectrally. Zoomed-in images of a single order from both the soliton and EO comb data (Figure 3b) show that individual comb lines are resolved at the NIRSPEC resolution of $R \sim 25,000$ and spaced approximately 4 pixels apart (0.1 nm) for the EO comb and 8 pixels (0.2 nm) for the soliton comb.

The soliton and EO comb time series data shown in Figure 3 consist of 450 data frames taken every 20 seconds over the course of a 2.5 hr interval when the telescope and instrument were in a quiescent state. The reduced echellograms were analyzed by fitting a Gaussian to each comb line (Figure 3c) to determine its pixel location (see Methods). For

this analysis we chose order #46 which spans 1.631 to 1.655 μm . The centroids of each comb line were determined across this 2.5 hr interval. The average drift for the entire order consisting of $N=122$ (225) lines in the soliton (EO comb) dataset, was computed with respect to the first frame in the time series and examined as a function of time to reveal drifts within NIRSPEC.

In the absence of external disturbances such as telescope-induced vibrations, the drift measured continuously in ~ 5 to 10 minute intervals over 2 hours was extremely regular and could be removed by a simple first-order fit. Subtracting the linear drift from the soliton data in the upper panel of Figure 3d results in the red dashed line (lower panel). Our calculation (see Methods) shows that this level of drift corresponds to 3-5 m s^{-1} precision in wavelength solution. Thus the ability to calibrate NIRSPEC at the few m s^{-1} level has been demonstrated using the soliton microcomb near-infrared technology. We emphasize that this wavelength precision is inherent to NIRSPEC's resolution and stability, and it is only the large number of LFC comb lines and their inherent high precision that have revealed the performance of NIRSPEC at this level (see Methods).

In routine astronomical operation, i.e. without an LFC, NIRSPEC has achieved radial velocity measurements at the 50 - 100 m/s level⁴³. Sources of uncertainty previously known or revealed during these observations include: changing illumination due to guiding errors of the star within the slit or shifting from the slit to the integrating sphere; short and long term drifts of 0.02-0.05 pixel due to internal vibrations and environmental effects; and sudden grating offsets due to telescope motions (0.25 pixel).

Observations of HD 187123 were bracketed by soliton measurements, but analysis of the stellar spectra and of telluric absorption lines within those spectra revealed variations at the 100 m s^{-1} level (0.025-0.05 pixel) which we attribute to the sources of wavelength shifts as described above. While planet detection could not be achieved, we were able to measure the two combs sequentially with respect to the arc lamps used for absolute wavelength calibration (see Extended Data Fig. 1).

A funded upgrade presently underway will enhance NIRSPEC's thermal and mechanical stability, and future upgrades would enable simultaneous observation of an LFC and a stellar image stabilized via a single mode fibre using Adaptive Optics. Finally, a new generation of spectrographs in development will utilize diffraction-limited Adaptive Optics imaging to enable $R > 100,000$ spectral resolution and enhanced image stability using single mode fibres. These new instruments will be able to take full advantage of the wavelength precision available with a new generation of microresonator astrocombs⁴⁴.

In summary, we report in-situ astronomical spectrograph calibrations with a soliton microcomb for the first time, which is an important milestone for future chip-based astrocomb research. The internal instrumental precision at the few m s^{-1} was limited by internal drifts of NIRSPEC and not by the performance of the soliton microcomb, which already possesses the desirable qualities of ~ 20 GHz mode spacing, low noise operation and short pulse generation. Rapidly progressing research in this field has resulted in microcomb spectral broadening and self-referencing with integrated photonics⁴⁵, as well as direct

generation at shorter wavelengths⁴⁶. These advances will greatly enhance the microcomb stability and bandwidth, and will eventually allow a new generation of astronomical instruments to attain the precision needed to detect the 10 cm s^{-1} RV signature of Earth-like exoplanets orbiting solar type stars at visible wavelengths. The current prototype system occupies approximately 1.3 m in a standard instrument rack, but significant effort towards system-level integration^{9,10}, could ultimately provide a microcomb system in a chip-integrated package with a footprint measured in centimetres. Such dramatic reduction in size is accompanied by reduced weight and power consumption, which would be an enabling factor for ubiquitous frequency comb precision RV calibrations, and other metrology applications in mobile and even space-borne^{47,48} instrumentation.

Note: The authors would like to draw the readers' attention to another microresonator astrocomb demonstration⁴⁹, which was reported while preparing this manuscript.

Methods

Silica microresonator and the device package.

The resonator is an 8 micron-thick disk resonator supporting whispering-gallery optical modes at the ~ 30 degree-wedged perimeter⁴². For transport to the observatory, the microresonator was mounted inside a brass package with FC/APC fibre connectors. The package was temperature-controlled using a thermoelectric cooler to stay within an operating range of 30 mK. The measured temperature stability was < 10 mK over an hour.

HCN reference laser.

Both centre-lock (reference) mode and side-lock (line narrowing) mode of the HCN reference laser (Clarity laser manufactured by Wavelength References, Inc.) were tested in the laboratory experiment. Stabilization of f_0 to a Rubidium-referenced local oscillator was possible by shifting entire soliton microcomb frequency using an acousto-optic frequency shifter when the reference laser was in side-lock mode. However, centre-lock mode, which provides better precision (< 1 MHz), is used and free-running f_0 is monitored for the on-site demonstration at the W.M. Keck Observatory. Because the comb precision of < 1 MHz is sufficient to detect the RV signature of HD 187123b, further improvement of the precision was not attempted to simplify the system as a first out-of-lab demonstration. In principle, full-stabilization of soliton microcomb is possible using a better optical frequency reference or via a self-referencing technique.

Spectral broadening of soliton microcomb.

The initial soliton microcomb out of the microresonator had $\sim \text{mW}$ optical power and was amplified above 1 Watt before entering the highly nonlinear optical fibre (HNLF). After spectral broadening, the high power peaks near the pump laser frequency are filtered out to prevent potential damage of the spectrograph. The broadened soliton microcomb had ~ 100 mW optical power and was further attenuated to $\sim \text{mW}$ before entering into the integrating sphere. The HNLF^{25,45,53}, spectral broadening medium, had three sections of fibre fusion-spliced together (5 metres of HNLF with -1.3 ps/nm/km normal dispersion, 60 centimetres of SMF 28, 2 metres of HNLF with 1.5 ps/nm/km anomalous dispersion). The first piece of

normal dispersion provides an efficient spectral broadening and a pulse output that can be temporally compressed with SMF 28. The anomalous HNLF section provides supercontinuum and dispersive-wave formation around 1200 nm.

Calibration of NIRSPEC.

We calculate the *relative* drift in the NIRSPEC wavelength solution, $\lambda(t)$, at time t by taking the average difference in centroid positions of each comb line ($j=1$ to N) in Order #46 at time t , $x_j(t)$, (Figure 3c) relative to the first frame in the time series, $x_j(t=0)$ as defined in eqn (1).

$$z(t) = \frac{1}{N} \sum_{j=1}^N (x_j(t) - x_j(t=0)). \quad (1)$$

$\lambda(t)$ with its associated uncertainty, $\sigma(t) / \sqrt{N}$, is shown in Figure 3d as measured by both the EO comb (black line) and the soliton microcomb (blue line). After subtracting the linear drift from the soliton data in Figure 3d, the soliton comb data reduced the wavelength drift over the two hour interval from 0.027 ± 0.002 pixel hr^{-1} (120 ± 10 m s^{-1} hr^{-1}) to zero ± 0.002 pixel hr^{-1} (± 10 m s^{-1} hr^{-1}). The 1σ residual around the linear fit in Figure 3d is 0.0034 pixels or 15 m s^{-1} . Other soliton-only datasets taken during these two days showed residuals as low as 0.0021 pixels after removal of a linear fit, or 9 m s^{-1} . These values represent the difference between two frames so that the wavelength precision in a single frame is $\sqrt{2}$ smaller or 10.6 m s^{-1} and 6.5 m s^{-1} .

The wavelength precision obtained above is based only on order #46, but there are four other orders in the echellogram with comparable amplitude and number of comb lines (Figure 3a). Adding in these other lines would improve the wavelength solution by $\sim \times 2$, or roughly 3-5 ms^{-1} .

The inset in Figure 3d demonstrates that the distribution of differences between comb-line centroids from one time step to the next after the subtraction of the mean shift, $(x_j(t) - x_j(t=0)) - \lambda(t)$ is well characterized by a Gaussian distribution. The precision in determining the frame-to-frame shift is dominated by the centroiding uncertainty (0.038 pixel in the differences, or $0.038 / \sqrt{2} = 0.027$ pixel in a single frame) and the total number of comb lines considered. The mean value of this distribution over the two hour period is 0.0001 ± 0.00079 pixels or 0.4 ± 3.4 m s^{-1} .

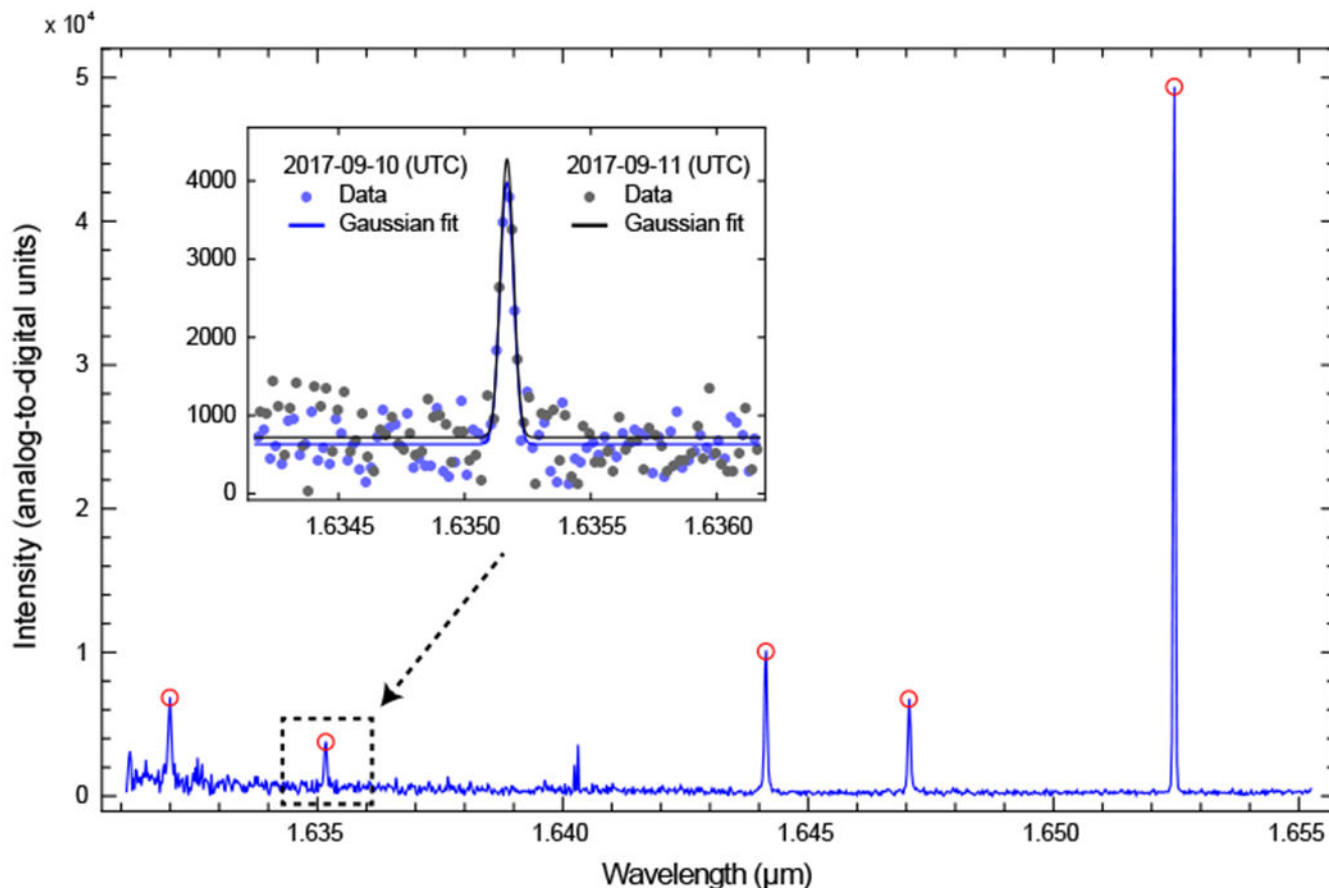
Performance limit of NIRSPEC.

A complete error-budget analysis for NIRSPEC shows that in an 900 sec observation, NIRSPEC could achieve (1, 1.6, 4.4) m/s on an $H=(6, 8, 10)$ mag M3 star after including the following effects: photon noise, simultaneous single mode fibre feeds of AO-stabilized starlight and the LFC, upgraded mechanical and thermal stability, stellar jitter and residual telluric effects.

Data availability.

The data that support the plots within this paper and other findings of this study are available from the corresponding author upon reasonable request.

Extended Data



Extended Data Fig. 1: Arc lamp data for absolute wavelength calibration.

NIRSPEC Arc lamps with lines of Kr, Ar, and Xe (<https://www2.keck.hawaii.edu/inst/nirspec/lines.html>) were used for the absolute wavelength calibration of the soliton comb lines, alternately configuring NIRSPEC to observe the arcs and the soliton. The figure shows a section of data from order 46. Gaussian fits were performed on 5 prominent lines from the two nights (blue and black data points in the inset). The average difference between the 5 line centroids is $0.98 \pm 1.3 \times 10^{-6}$ nm, which corresponds to 0.041 ± 0.025 pixel. This shift is consistent with short term drifts seen through the two nights.

Acknowledgments

We gratefully acknowledge Josh Schlieder, Prof. Andrew Howard, Fred Hadaegh and the support of the entire Keck summit team. We thank David Carlson and Henry Timmers for preparing the highly nonlinear optical fiber. The authors wish to recognize and acknowledge the very significant cultural role and reverence that the summit of Mauna Kea has always had within the indigenous Hawaiian community. The data presented herein were obtained at the W.M. Keck Observatory, which is operated as a scientific partnership among the California Institute of Technology, the University of California and the National Aeronautics and Space Administration. The Observatory

was made possible by the generous financial support of the W.M. Keck Foundation. This paper made use of data available in the NASA Exoplanet Archive and the Keck Observatory Archive. S.D. and S.P. acknowledge support from NIST. K.V., M.G.S., X.Y. and Y.H.L. thank the Kavli Nanoscience Institute and the National Aeronautics and Space Administration for support under KJV.JPLNASA-1-JPL.1459106. This research was carried out at the Jet Propulsion Laboratory and the California Institute of Technology under a contract with the National Aeronautics and Space Administration and funded through the JPL Research and Technology Development.

References

1. Kasting JF, Whitmire DP & Reynolds RT Habitable zones around main sequence stars. *Icarus* 101, 108–128 (1993). [PubMed: 11536936]
2. Diddams SA The evolving optical frequency comb. *JOSA B* 27, B51–B62 (2010).
3. Herr T et al. Temporal solitons in optical microresonators. *Nat. Photonics* 8, 145–152 (2014).
4. Yi X, Yang QF, Yang KY, Suh MG & Vahala K Soliton frequency comb at microwave rates in a high-q silica microresonator. *Optica* 2, 1078–1085 (2015).
5. Brasch V et al. Photonic chip-based optical frequency comb using soliton cherenkov radiation. *Science* 351, 357–360 (2016). [PubMed: 26721682]
6. Wang PH et al. Intracavity characterization of micro-comb generation in the single-soliton regime. *Opt. Express* 24, 10890–10897 (2016). [PubMed: 27409909]
7. Joshi C et al. Thermally controlled comb generation and soliton modelocking in microresonators. *Opt. Lett* 41, 2565–2568 (2016). [PubMed: 27244415]
8. Grudinin IS et al. High-contrast kerr frequency combs. *Optica* 4, 434–437 (2017).
9. Spencer DT et al. An optical-frequency synthesizer using integrated photonics. *Nature* 557, 81–85 (2018). [PubMed: 29695870]
10. Stern B, Ji X, Okawachi Y, Gaeta AL & Lipson M Fully integrated ultra-low power kerr comb generation. *arXiv preprint arXiv:1804.00357* (2018).
11. Perryman M The exoplanet handbook (Cambridge University Press, 2011).
12. Pepe F, Ehrenreich D & Meyer MR Instrumentation for the detection and characterization of exoplanets. *Nature* 513, 358–366 (2014). [PubMed: 25230658]
13. Wilken T et al. A spectrograph for exoplanet observations calibrated at the centimetre-per-second level. *Nature* 485, 611–614 (2012). [PubMed: 22660320]
14. Jones DJ et al. Carrier-envelope phase control of femtosecond mode-locked lasers and direct optical frequency synthesis. *Science* 288, 635 (2000). [PubMed: 10784441]
15. Murphy MT et al. High-precision wavelength calibration of astronomical spectrographs with laser frequency combs. *Mon. Notices Royal Astron. Soc* 380, 839–847 (2007).
16. Li CH et al. A laser frequency comb that enables radial velocity measurements with a precision of 1 cm s⁻¹. *Nature* 452, 610–612 (2008). [PubMed: 18385734]
17. Braje DA, Kirchner MS, Osterman S, Fortier T & Diddams S Astronomical spectrograph calibration with broad-spectrum frequency combs. *The Eur. Phys. J. D* 48, 57–66 (2008).
18. Glenday AG et al. Operation of a broadband visible-wavelength astro-comb with a high-resolution astrophysical spectrograph. *Optica* 2, 250–254 (2015).
19. McCracken RA, Charsley JM & Reid DT A decade of astrocombs: recent advances in frequency combs for astronomy. *Opt. Express* 25, 15058–15078 (2017). [PubMed: 28788939]
20. Steinmetz T et al. Laser frequency combs for astronomical observations. *Science* 321, 1335–1337 (2008). [PubMed: 18772434]
21. Murata H, Morimoto A, Kobayashi T & Yamamoto S Optical pulse generation by electrooptic-modulation method and its application to integrated ultrashort pulse generators. *IEEE J. Sel. Top. Quantum Electron* 6, 1325–1331 (2000).
22. Huang C, Jiang Z, Leaird D & Weiner A High-rate femtosecond pulse generation via line-by-line processing of phase-modulated cw laser frequency comb. *Electron. Lett* 42, 1 (2006).
23. Yi X et al. Demonstration of a near-ir line-referenced electro-optical laser frequency comb for precision radial velocity measurements in astronomy. *Nat. Commun* 7 (2016).
24. Beha K et al. Electronic synthesis of light. *Optica* 4, 406–411 (2017).

25. Carlson DR et al. Ultrafast electro-optic light with subcycle control. *Science* 361, 1358–1363 (2018). [PubMed: 30262499]
26. Metcalf AJ et al. Infrared astronomical spectroscopy for radial velocity measurements with 10 cm/s precision In *CLEO: Science and Innovations*, JTh5A–1 (Optical Society of America, 2018).
27. DelHaye P et al. Optical frequency comb generation from a monolithic microresonator. *Nature* 450, 1214–1217 (2007). [PubMed: 18097405]
28. Kippenberg TJ, Holzwarth R & Diddams S Microresonator-based optical frequency combs. *Science* 332, 555–559 (2011). [PubMed: 21527707]
29. Kippenberg T, Spillane S & Vahala K Kerr-nonlinearity optical parametric oscillation in an ultrahigh-q toroid microcavity. *Phys. Rev. Lett* 93, 083904 (2004). [PubMed: 15447188]
30. Wabnitz S Suppression of interactions in a phase-locked soliton optical memory. *Opt. Lett* 18, 601–603 (1993). [PubMed: 19802213]
31. Leo F et al. Temporal cavity solitons in one-dimensional kerr media as bits in an all-optical buffer. *Nat. Photonics* 4, 471–476 (2010).
32. Suh MG, Yang QF, Yang KY, Yi X & Vahala KJ Microresonator soliton dual-comb spectroscopy. *Science* 354, 600–603 (2016). [PubMed: 27738017]
33. Dutt A et al. On-chip dual-comb source for spectroscopy. *Sci. Adv* 4, e1701858 (2018). [PubMed: 29511733]
34. Pavlov N et al. Soliton dual frequency combs in crystalline microresonators. *Opt. Lett* 42, 514–517 (2017). [PubMed: 28146515]
35. Trocha P et al. Ultrafast optical ranging using microresonator soliton frequency combs. *Science* 359, 887–891 (2018). [PubMed: 29472477]
36. Suh MG & Vahala KJ Soliton microcomb range measurement. *Science* 359, 884–887 (2018). [PubMed: 29472476]
37. Marin-Palomo P et al. Microresonator-based solitons for massively parallel coherent optical communications. *Nature* 546, 274–279 (2017). [PubMed: 28593968]
38. Feng YK et al. The california planet survey iv: A planet orbiting the giant star hd 145934 and updates to seven systems with long-period planets. *The Astrophys. J* 800, 22 (2015).
39. Mahadevan S et al. The habitable-zone planet finder: a stabilized fiber-fed nir spectrograph for the hobby-eberly telescope In *Ground-based and Airborne Instrumentation for Astronomy IV*, vol. 8446, 84461S (International Society for Optics and Photonics, 2012).
40. Kotani T et al. Infrared doppler instrument (ird) for the subaru telescope to search for earth-like planets around nearby m-dwarfs In *Ground-based and Airborne Instrumentation for Astronomy V*, vol. 9147, 914714 (International Society for Optics and Photonics, 2014).
41. McLean IS et al. Design and development of nirspec: a near-infrared echelle spectrograph for the keck ii telescope In *Infrared Astronomical Instrumentation*, vol. 3354, 566–579 (International Society for Optics and Photonics, 1998).
42. Lee H et al. Chemically etched ultrahigh-q wedge-resonator on a silicon chip. *Nat. Photonics* 6, 369–373 (2012).
43. Blake CH, Charbonneau D & White RJ The nirspec ultracool dwarf radial velocity survey. *The Astrophys. J* 723, 684 (2010).
44. Crepp JR et al. ilocator: a diffraction-limited doppler spectrometer for the large binocular telescope In *Ground-based and Airborne Instrumentation for Astronomy VI*, vol. 9908, 990819 (International Society for Optics and Photonics, 2016).
45. Lamb ES et al. Optical-frequency measurements with a kerr microcomb and photonic-chip supercontinuum. *Phys. Rev. Appl* 9, 024030 (2018).
46. Lee SH et al. Towards visible soliton microcomb generation. *Nat. Commun* 8 (2017).
47. Lezius M et al. Space-borne frequency comb metrology. *Optica* 3, 1381–1387 (2016).
48. Plavchan P et al. Earthfinder: A precise radial velocity probe mission concept for the detection of earth-mass planets orbiting sun-like stars. *arXiv preprint arXiv:1803.03960* (2018).
49. Obrzud E et al. A microphotonic astrocomb. *Nat. Photon* 10.1038/s41566-018-0309-y (2018).
50. Cai M, Painter O & Vahala KJ Observation of critical coupling in a fiber taper to a silica-microsphere whispering-gallery mode system. *Phys. Rev. Lett* 85, 74 (2000). [PubMed: 10991162]

51. Spillane S, Kippenberg T, Painter O & Vahala K Ideality in a fiber-taper-coupled microresonator system for application to cavity quantum electrodynamics. *Phys. Rev. Lett* 91, 043902 (2003). [PubMed: 12906659]
52. Yi X, Yang QF, Youl K & Vahala K Active capture and stabilization of temporal solitons in microresonators. *Opt. Lett* 41, 2037–2040 (2016). [PubMed: 27128068]

Methods references

53. Cole D, Beha K, Diddams S & Papp S, Octave-spanning supercontinuum generation via microwave frequency multiplication. *Journal of Physics: Conference Series*. 723, 012035 (2016).

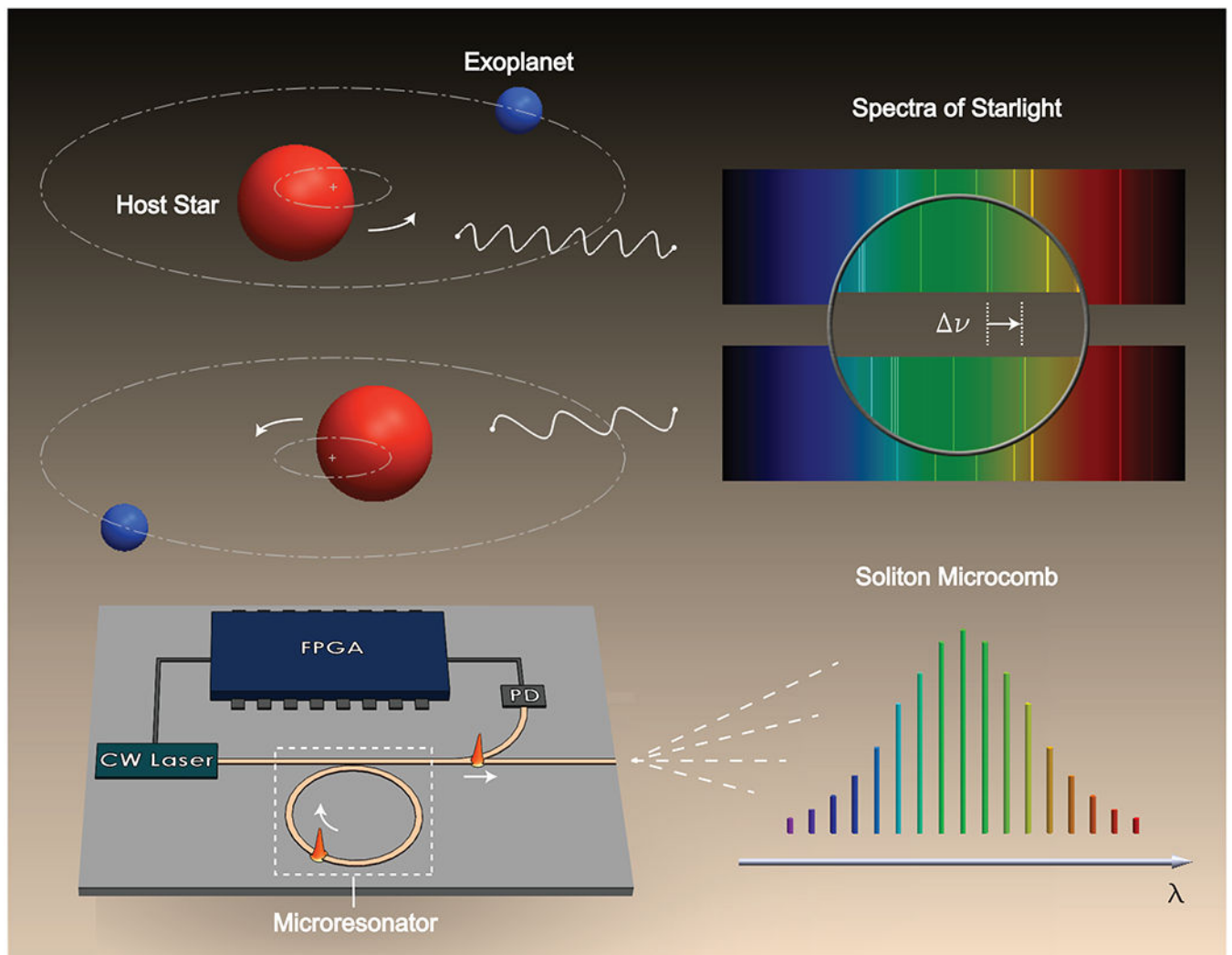


FIG. 1: Concept of a microresonator astrocomb.

While the host star (red sphere) and exoplanet (blue sphere) orbit their common centre of mass, light waves leaving the star experience a weak Doppler shift. The frequency shift (ν) of the stellar spectral lines are measured with a spectrograph calibrated using an evenly spaced comb of frequencies. Here, the comb of frequencies is produced by soliton emission from a microresonator, which can be potentially integrated with a continuous-wave (CW) laser, a photodetector (PD) and a field-programmable gate array (FPGA) on a chip-scale device.

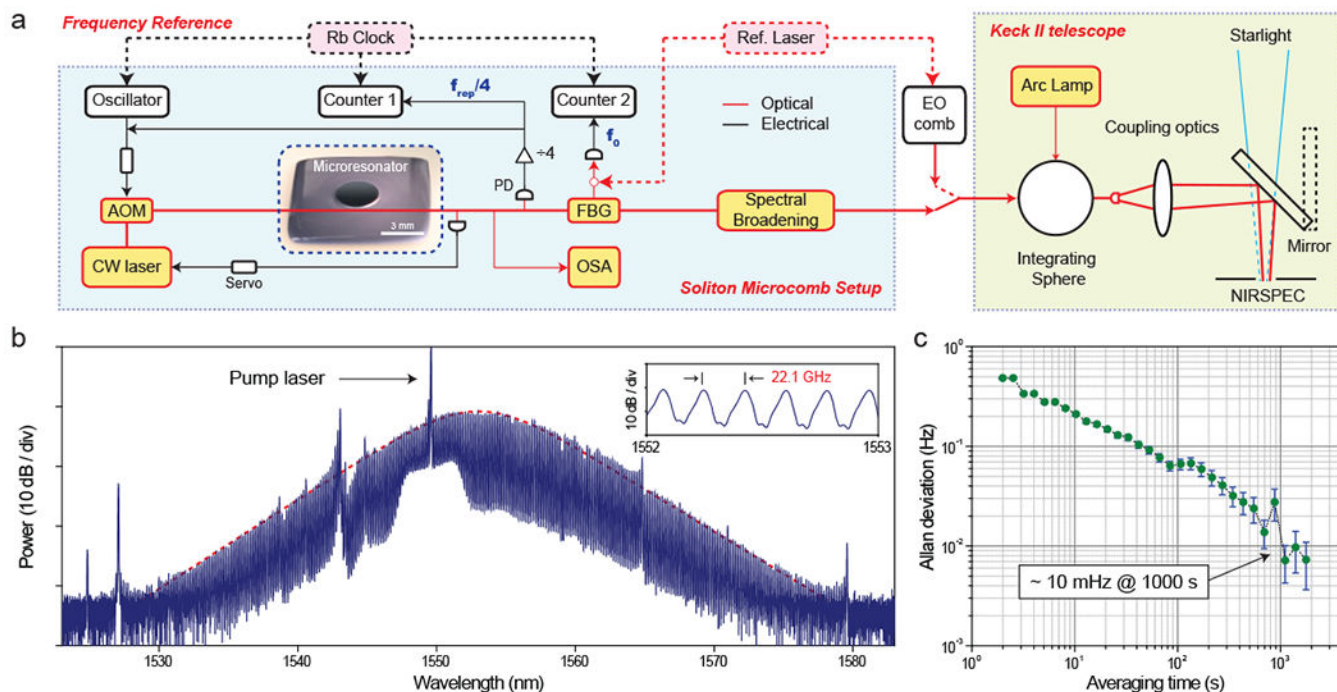


FIG. 2: Experimental schematic and atomic/molecular line-referenced soliton microcomb.

(a) Continuous-wave (CW) fibre laser is coupled into a silica microresonator via a tapered fibre coupler^{50,51}. An acousto-optic modulator (AOM) controls pump power. The soliton microcomb is long-term stabilized by servo control of the pump laser frequency to hold a fixed soliton average power⁵². The comb power is also tapped to detect and stabilize the repetition frequency (f_{rep}). After dividing by 4, f_{rep} is frequency-locked to an oscillator and monitored using a frequency counter. The depicted control electronics can be potentially replaced by a compact FPGA as shown in Fig.1. A rubidium (Rb) clock provides an external frequency reference. The frequency offset (f_0) of a soliton comb line is measured relative to a reference laser (stabilized to HCN at 1559.9 nm). This comb line is filtered-out by a fibre Bragg grating (FBG) filter and heterodyned with the reference laser. Finally, the soliton microcomb is spectrally broadened and sent to the integrating sphere of the NIRSPEC instrument on the Keck II telescope for spectrograph calibration. As a cross check, an EO comb (instead of soliton microcomb) is also used. (b) Optical spectrum of the soliton microcomb. The hyperbolic-secant-square fit (red dotted curve) indicates that the soliton pulse width is 145 fs. Inset : Zoom-in of the spectra showing 22.1 GHz line spacing. (c) Allan deviation of the frequency-locked $f_{rep}/4$. PD : photodetector, OSA : optical spectrum analyzer.

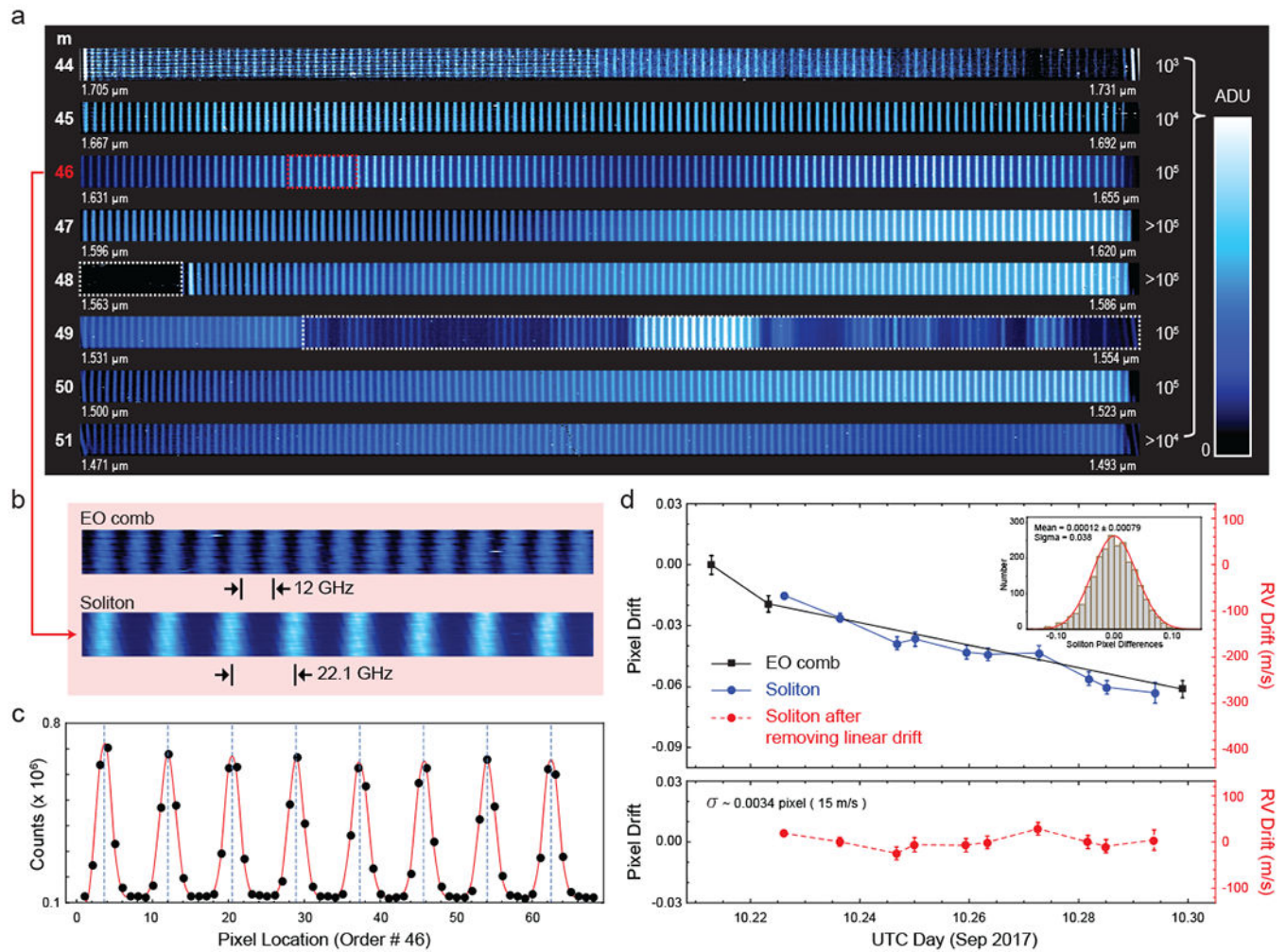


FIG. 3: Data from testing at Keck II.

(a) Image of soliton comb projected onto the NIRSPEC from the echelle orders 44 to 51. Soliton emission (white dashed box) has been strongly filtered to prevent potential damage of the spectrograph. ADU: Analogue-to-Digital Units. (b) A zoom-in of the Echelle order 46 (red dashed box in panel a) of the EO comb (upper) and soliton (lower). (c) Gaussian profiles of 8 adjacent soliton comb lines in Order #46 are shown (see Methods). (d) Upper panel shows average centroid drift within Order #46 relative to the first frame in the time series with both the soliton (blue) and EO combs (black) with the telescope in a quiescent configuration on 9/10/2017 UTC. The EO comb data bracketing the soliton comb data shows the drift of the NIRSPEC wavelength scale. The lower panel shows the NIRSPEC drift after subtracting a linear trend and gives a residual of 0.0034 pixel which corresponds to approximately 15 m s^{-1} in a single order. The inset in the upper panel shows that the distribution of centroid differences is well defined by a Gaussian distribution (see Methods). As discussed in the text the final wavelength calibration across the entire echellogram would be $< 5 \text{ m s}^{-1}$.